Light Metals 2014
Edited by: John Grandfield
TMS (The Minerals, Metals & Materials Society), 2014

AN EXPERIMENTAL AND MODELING INVESTIGATION ON HIGH-RATE FORMABILITY OF ALUMINUM

Aashish Rohatgi[1], Richard W. Davies[1], Elizabeth V. Stephens[1], Ayoub Soulami[1] and Mark T. Smith[1]
[1]Pacific Northwest National Laboratory (PNNL), 902 Battelle Blvd.
P.O. Box 999, Richland, WA 99352, USA

Keywords: Formability, High Strain-Rate, Electro-hydraulic Forming, Digital Image Correlation

Abstract

This work describes the integrated experimental and modeling effort at PNNL to enhance the room-temperature formability of aluminum alloys by taking advantage of formability improvements generally associated with high-strain-rate forming. Al alloy AA5182-O sheets were deformed in near plane-strain conditions at strain-rates exceeding 1000 /s using the electrohydraulic forming (EHF) technique, and at quasi-static strain-rates via a bulge test. A novel capability, combining high-speed imaging with digital image correlation technique, was developed to quantify the deformation history during high-rate forming. Sheet deformation under high rates was modeled in Abaqus and validated with experimentally determined deformation data. The experimental results show a ~2.5x increase in formability at high rates, relative to quasi-static rates, under a proportional loading path that was verified by the experimental data. The model shows good correlation with the experimentally determined strain path. It is anticipated that such integrated experimental and modeling work will enable room-temperature forming of Al and industrial implementation of high-rate forming processes.

Introduction

The goal of this work is to enable aluminum sheet components to replace steel in automotive applications as a means to reduce the weight of the vehicle and lead to reduced fuel consumption and green-house gas emissions. However, Al has much lower formability than mild steel [1] at room-temperature (see Fig. 1) and its poor formability, therefore, is an obstacle in cost-effective automotive weight reduction through replacement of steel with aluminum sheet components. In order to address this issue, our efforts have been focused on developing an integrated experimental and modeling approach to enhance the room-temperature formability of Al alloy sheets through the use of high-rate pulse-pressure forming (PPF) processes. In specific, this research is investigating the electro-hydraulic forming (EHF) process wherein an intense pressure-pulse is generated under water and used to form sheet metals into single-sided dies to produce contoured shape. The forming event duration is on the order of several hundred microseconds with strain-rates from ~10^2 /s to exceeding 10^3 /s. Such high-rates have been shown to enhance the formability of aluminum and other sheet metals and the prior literature has been reviewed by Rohatgi et al. [2]. In the literature, experimental techniques such as high-speed imaging [3], Photon Doppler Velocimetry [4], laser-shadowing [5] etc. have been used to interrogate high-rate forming processes. However, these techniques are limited to sheet displacement and velocity information and lack the strain-rate and strain-path information that is critical to understanding the mechanisms behind enhanced formability. To address this information gap, our group at PNNL has developed a unique experimental

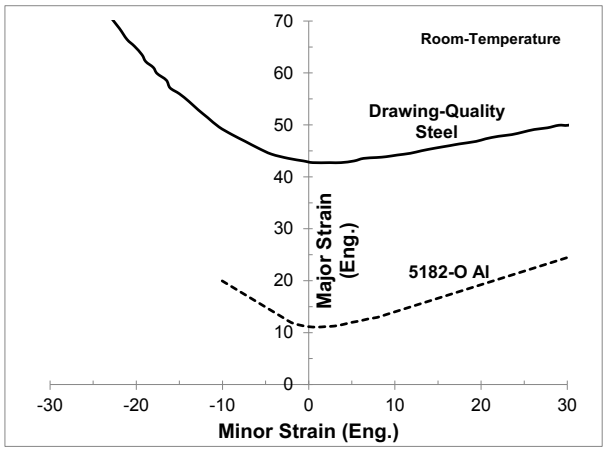

Figure 1. Room-temperature forming limit curves (FLC) for a drawing quality steel [1] and 5182-O Al sheet (vendor provided data).

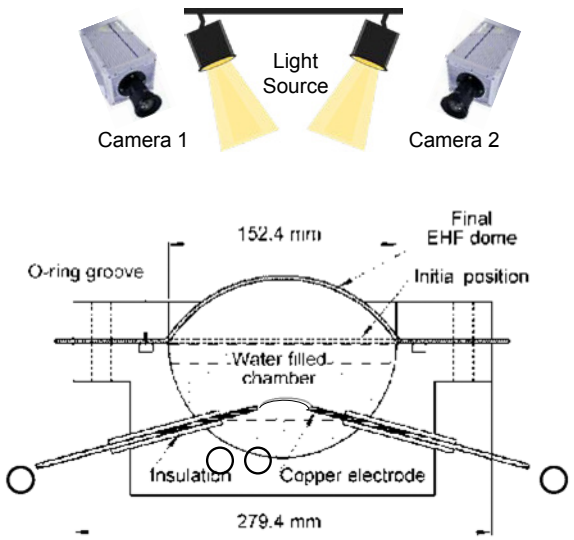

Figure 2. A schematic of EHF and high-speed imaging setup.

capability, combining high-speed imaging and digital image correlation (DIC), that can quantify the deformation history (strain, strain-rate, velocity, displacement) during high-rate forming [2, 6-8]. The current work provides a snap-shot of the experimentally determined deformation history associated with enhanced formability in 5182-O Al at high strain-rates. Additionally, a numerical model of high-rate forming is also described and its predictions compared with the experimentally determined data.

Experimental Procedure

AA5182-O sheets, 1 mm thick, were free-formed (i.e. without a die) into domes via the EHF technique. Fig. 2 shows a schematic of PNNL's EHF and high-speed imaging setup. The test specimen geometry is shown in Fig. 3 and is termed as the plane-strain or single-ligament geometry. During testing, the test specimen and an underlying driver sheet were clamped on the EHF die. The driver sheet was a 1 mm thick solid sheet (i.e. without any elliptical cut-outs) of 5182-O Al. The pressure pulse was created by charging a capacitor bank to the desired voltage (8500 V in the present work) and then discharging the stored energy as high-intensity currents between the copper electrodes through a 0.3 mm diameter copper wire (connecting the electrodes). The pressure-pulse generated in the water resulted in the deformation of the test sheet (and the driver sheet). One side of the test sheets was painted with a speckle pattern while the other side was etched with a square grid pattern (2.54 mm x 2.54 mm). The in-situ sheet deformation was imaged using a pair of Photron cameras at a frame rate of upto 75,000 per second and at an image resolution of upto 320 x 264 pixels. The quantification of sheet deformation history (strain, strain-rate, velocity, displacement) was performed using the DIC technique by analyzing the speckle pattern, painted on the test sheets, using commercial software (Vic-3d, version 2009.1.0, from Correlated Solutions, Inc.). The strain and strain-rate determined by the software are presented in Lagrangian formulation unless stated otherwise. The deformation data (strain, strain-rate) is presented here as contour plots as well as data determined at a distinct location on the sheet. A quasi-static version of the above described forming experiment was carried out by gradually pressurizing the water (~240 kPa/s) in the die until the sheet failed. Cameras and DIC imaging were not used for the quasi-static tests. Post-deformation strains for both, high-rate and quasi-static tests, were quantified by analyzing the deformed grid using an image analysis software (ASAME, version 4.1 by ASAME technology LLC). Additional details on the test configuration including EHF and imaging setup etc. are given elsewhere [2, 6-8].

The sheet deformation was modeled using commercial finite element software Abaqus and employing axi-symmetric 2D models with element size of ~1 mm. Johnson-Cook constitutive model was used to model the flow stress of the material and the equation parameters were determined using quasi-static (0.001-0.1 /s) and high-rate (1000-2400 /s) uniaxial tension tests. The pressure-pulse was modeled as an exponentially decaying pulse of the form:

$$P(t) = P_0.Np.(t/\theta)^a.exp(-bt/\theta) \quad (1)$$

where P is the pressure, t is the time, P_0 is the peak pressure amplitude (= 7 MPa), and Np (=1.28), θ (=150 microseconds), a (= 0.089), and b (=0.53) are various constants. See Fig. 4 and [2] for additional details.

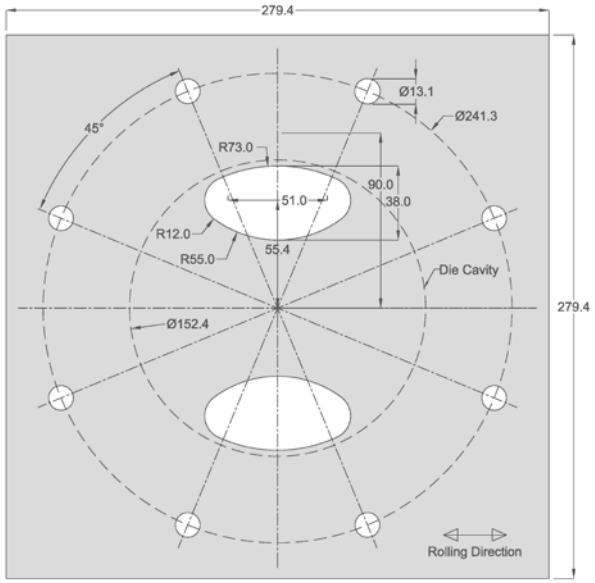

Figure 3. Drawings of the plane-strain/single-ligament specimen geometry tested in this work; the white spaces are elliptical cut-outs in the sheet, designed to obtain a state of near-plane-strain in the center of the sheet.

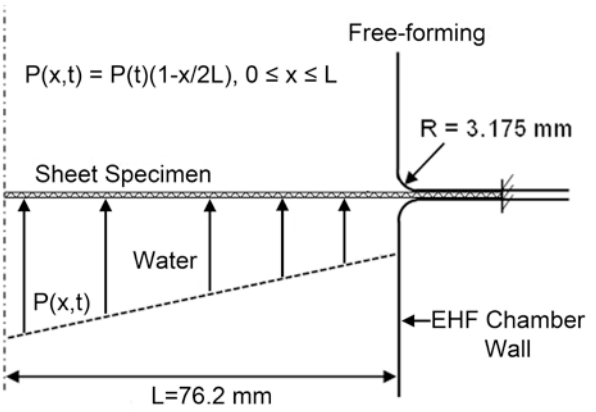

Figure 4. Spatial distribution of the pressure pulse used to model the free-forming of samples.

Results and Discussion

Fig. 5a shows an image of the EHF-formed plane-strain specimen (the underlying driver sheet is not shown). The specimen fractured across the center. Once initiated, it is not possible to "stop" the pressure-pulse at the moment of specimen fracture. Hence, the two halves of the specimen were pushed further apart by the still-deforming driver sheet. Fig. 5b shows the strain-rate contours near the instance when failure occurred. The data shows that the Lagrangian strain-rate is ~6000 /s just before fracture at strains ranging from ~0.50 to 0.66 (Fig. 5c). See [2] for additional details.

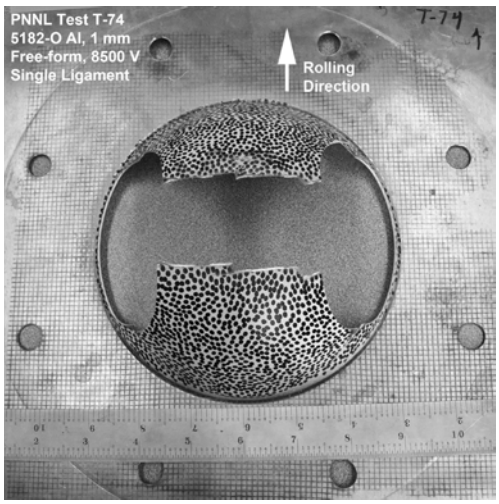

(a)

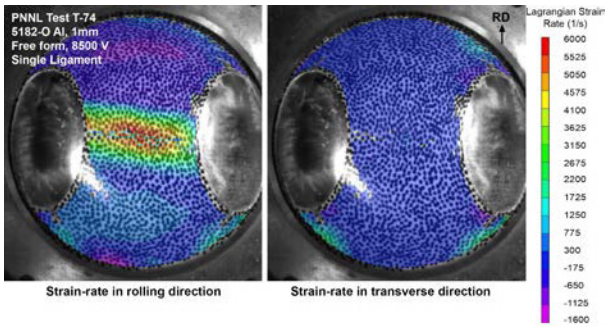

(b)

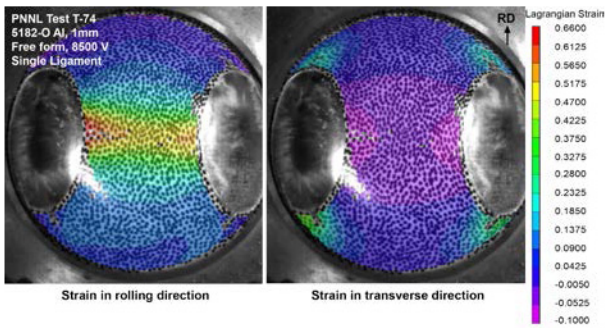

(c)

Figure 5. EHF formed plane-strain/single-ligament specimen showing (a) top view, (b) strain-rate contours, and (c) strain contours. The rolling direction corresponds to the major strain in Figures 7 and 8.

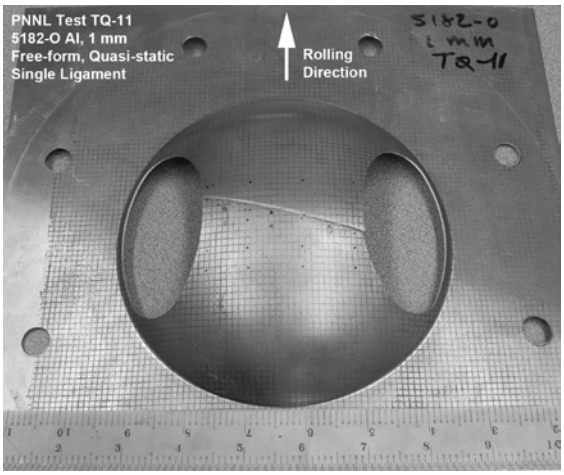

(a)

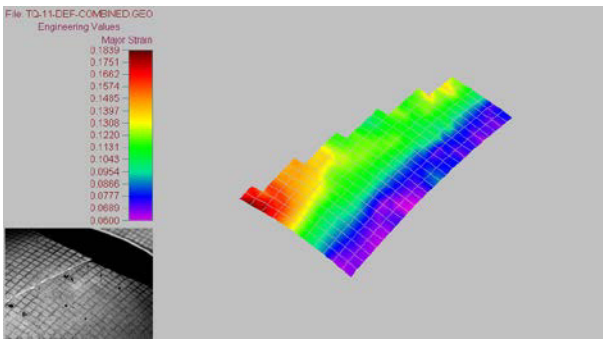

(b)

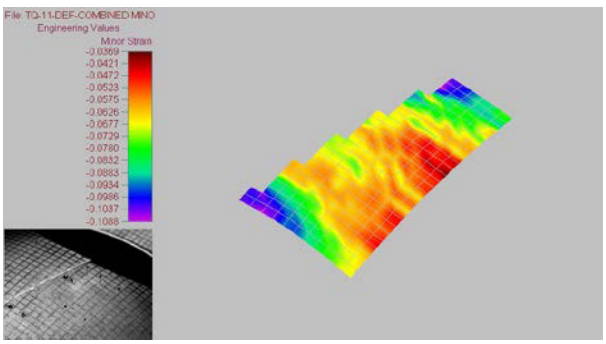

(c)

Figure 6. Quasi-statically deformed plane-strain/single-ligament specimen showing (a) top view, (b) post-deformation major (along rolling direction) engineering strain, and (b) post-deformation minor (in transverse direction) engineering strains.

Fig. 6a shows an image of the quasi-statically bulge-formed plane-strain specimen. Similar to the EHF-formed specimen shown in Fig. 5, the quasi-static failure also occurred across the center. However, unlike the EHF process, it was possible to stop the pressurization upon specimen failure, and hence, the sheets have not been forced apart as they were in the EHF specimen. The failure occurred at a pressure of ~10 MPa (i.e. in ~40 seconds). Hence, the quasi-static deformation occurred at a nominal rate that is nominally ~10^5 orders of magnitude lower than the EHF test duration (~400 microseconds). Fig. 6b and 6c show the major and minor strains measured near the fracture region using the conventional grid-analysis method. The data shows that majority of the safe strains are ~14% or less while the safe minor strains are in the range of -6% to -8%.

The safe and incipient strain data from the high-rate and quasi-static tests have been plotted on the FLD in Fig. 7. The strain-grid

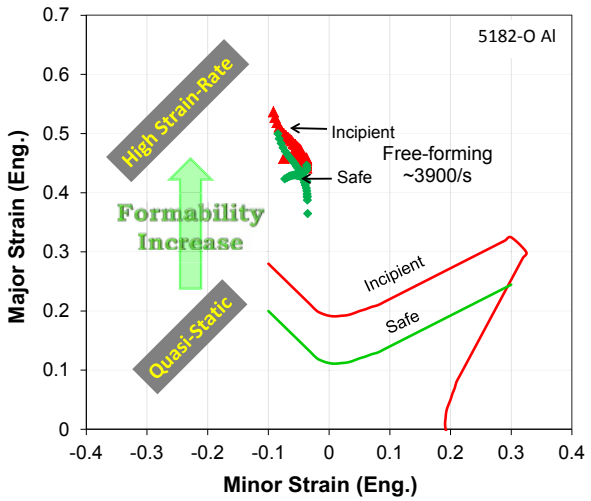

Figure 7. Forming limit diagram (FLD) of 5182-O Al showing the EHF strains and the vendor-provided quasi-static forming limit curves (FLC).

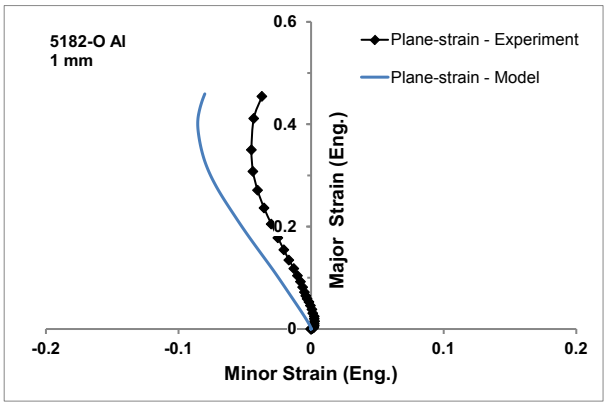

Figure 8. Model predicted and experimentally measured strain path for the plane-strain specimen.

data from the quasi-statically deformed specimen (Fig. 6b and 6c) is close to the vendor-provided FLC and hence, have been omitted from the FLD in Fig. 7. A comparison of the high-rate strains and quasi-static FLC in Fig. 7 demonstrates a ~2.5X enhancement in the formability due to high strain-rates achieved during EHF. The peak strain-rate along the major strain direction and corresponding to the formability enhancement is ~3900 /s (engineering).

Fig. 8 plots the experimentally determined major strain at the apex of the plane-strain specimen as a function of the corresponding minor strain. Essentially, this curve describes the strain-path that the corresponding location on the specimen undergoes through during the course of the deformation. Hence, the (0,0) data represents the start of the test and (~0.5,~-0.05) represents the end of the test and intervening data points represent the progress of deformation in the sample. The plot in Fig. 8 shows that for the majority of the duration, the strain-path followed by the sample is proportional, i.e. the ratio of major to minor strain is constant. It should be noted that strictly speaking, the strain path needs to be proportional for the FLD to be considered valid. This proportionality requirement stems from the observation that the formability of a material is a function of strain path. One example of path-dependent formability is the formability enhancement observed during incremental forming processes [9]. Hence, the fact that this work has experimentally demonstrated the EHF strain path to be proportional implies that the demonstrated formability enhancement during EHF, relative to quasi-static FLC, is indeed a valid comparison and not a strain path effect. The formability enhancement under a proportional strain-path demonstrated here is in contrast to existing literature where either (i) forming occurs inside a die and a proportional strain path is not maintained when the sheet impacts the die (e.g. [10, 11]), or (ii) a proportional path is implicitly assumed but not experimentally verified (e.g. [12, 13]). Fig. 8 also shows a good agreement between the predicted and experimentally determined strain-path. The slight discrepancy between the two is likely due to the difference in the assumed and actual pressure-pulse profile and due to limitations of the Johnson-Cook model to correctly predict the sheet behavior at strain-rates (>2400 /s) beyond which it was calibrated for (1000-2400 /s).

Conclusions

The deformation history and formability of AA5182-O sheets, formed by EHF technique at room-temperature, was determined using a novel combination of high-speed imaging and DIC technique. The high-rate deformation behavior of the sheet was modeled using finite element software (Abaqus) and compared. Based on the results of this work, the following conclusions are made:

1) High-rate free-forming via the EHF technique was shown to enhance the room-temperature formability of AA5182-O, under near-plane-strain conditions, by ~2.5x relative to its formability under quasi-static forming.
2) The peak strain-rate associated with formability enhancement was measured to be ~3900 /s in the major strain direction.
3) The formability enhancement was achieved under a proportional strain-path and this proportionality was demonstrated experimentally.
4) The model predicted strain path was in good agreement with that determined experimentally, validating the approach and assumptions used in its development.

Acknowledgement

The Pacific Northwest National Laboratory is operated by Battelle Memorial Institute for the U.S. Department of Energy under contract DE-AC05-76RL01830. This work was sponsored by J. Carpenter, C. Schutte and W. Joost in association with the U.S. Department of Energy, Office of Vehicle Technologies, as part of the Lightweight Materials program. The authors would like to thank the U.S. automotive industry partners for their suggestions in the course of this work. Technical support by J. Johnson (Bonneville Power Administration), A. Tofts and H. Schreier (Correlated Solutions), and PNNL staff G.L. Vanarsdale, M.E. Dahl, and K.F. Mattlin, is gratefully acknowledged.

References

[1] K.S. Raghavan, Metallurgical and Materials Transactions A-Physical Metallurgy and Materials Science, 26 (1995) 2075-2084.

[2] A. Rohatgi, A. Soulami, E.V. Stephens, R.W. Davies, M.T. Smith, J. Mater. Process. Technol., In Press, http://dx.doi.org/10.1016/j.jmatprotec.2013.07.015 (2013).
[3] T. Tobe, M. Kato, H. Obara, Bulletin of the JSME-Japan Society of Mechanical Engineers, 27 (1984) 130-135.
[4] J.R. Johnson, G. Taber, A. Vivek, Y. Zhang, S. Golowin, K. Banik, G.K. Fenton, G.S. Daehn, Steel Research International, 80 (2009) 359-365.
[5] M. Badelt, C. Beerwald, A. Brosius, M. Kleiner, in: ESAFORM 2003 - 6th International Conference on Material Forming, Salerno, Italy, 2003, pp. 123-126.
[6] A. Rohatgi, E.V. Stephens, A. Soulami, R.W. Davies, M.T. Smith, in: R. Kolleck (Ed.) International Deep Drawing Group (IDDRG), Graz, Austria, 2010, pp. 441-450.
[7] A. Rohatgi, E.V. Stephens, A. Soulami, R.W. Davies, M.T. Smith, J. Mater. Process. Technol., 211 (2011) 1824-1833.
[8] A. Rohatgi, E.V. Stephens, R.W. Davies, M.T. Smith, A. Soulami, S. Ahzi, J. Mater. Process. Technol., 212 (2012) 1070-1079.
[9] W.C. Emmens, D.H. van der Weijde, A.H. van den Boogard, in: IDDRG 2009 International Conference, IDDRG, Golden, CO, USA, 2009, pp. 773-784.
[10] J. Imbert, M. Worswick, S. Winkler, S. Golovashchenko, V. Dmitriev, in: SAE World Congress, Paper 2005-01-0082, SAE International, Detroit, Michigan, USA, 2005.
[11] J.M. Imbert, S.L. Winkler, M.J. Worswick, D.A. Oliveira, S. Golovashchenko, J. Eng. Mater. Technol. Trans. ASME, 127 (2005) 145-153.
[12] A.A. Tamhane, M.M. Altynova, G.S. Daehn, Scr. Mater., 34 (1996) 1345-1350.
[13] J.D. Thomas, M. Seth, G.S. Daehn, J.R. Bradley, N. Triantafylldis, Acta Materialia, 55 (2007) 2863-2873.